Increasing the length of progerin's isoprenyl anchor does not worsen bone disease or survival in mice with Hutchinson-Gilford progeria syndrome

Brandon S. J. Davies,* Shao H. Yang,* Emily Farber,* Roger Lee,* Suzanne B. Buck,** Douglas A. Andres,†† H. Peter Spielmann,†† Brian J. Agnew,** Fuyuhiko Tamanoi,§ Loren G. Fong,[1]* and Stephen G. Young[1]*,†

Department of Medicine,* Human Genetics,† and Microbiology, Immunology, and Molecular Genetics,§ David Geffen School of Medicine, University of California, Los Angeles, CA 90095; Molecular Probes-Invitrogen,** Eugene OR 97402; and Department of Molecular and Cellular Biochemistry,†† University of Kentucky, Lexington, KY 40536

Abstract Hutchinson-Gilford progeria syndrome (HGPS) is caused by the synthesis of a truncated prelamin A, commonly called progerin, that contains a carboxyl-terminal farnesyl lipid anchor. The farnesyl lipid anchor helps to target progerin to membrane surfaces at the nuclear rim, where it disrupts the integrity of the nuclear lamina and causes misshapen nuclei. Several lines of evidence have suggested that progerin's farnesyl lipid anchor is crucial for the emergence of disease phenotypes. Because a geranylgeranyl lipid is ~45-fold more potent than a farnesyl lipid in anchoring proteins to lipid membranes, we hypothesized that a geranylgeranylated version of progerin might be more potent in eliciting disease phenotypes. To test this hypothesis, we used gene targeting to create mice expressing geranylgeranylated progerin ($Lmna^{ggHG/+}$). We then compared $Lmna^{ggHG/+}$ mice, side-by-side, with otherwise identical mice expressing farnesylated progerin ($Lmna^{HG/+}$). Geranylgeranylation of progerin in $Lmna^{ggHG/+}$ cells and farnesylation of progerin in $Lmna^{HG/+}$ cells was confirmed by metabolic labeling. Contrary to our expectations, $Lmna^{ggHG/+}$ mice survived longer than $Lmna^{HG/+}$ mice. The $Lmna^{ggHG/+}$ mice also exhibited milder bone disease. The steady-state levels of progerin, relative to lamin C, were lower in $Lmna^{ggHG/+}$ mice than in $Lmna^{HG/+}$ mice, providing a potential explanation for the milder disease in $Lmna^{ggHG/+}$ mice.— Davies, B. S. J., S. H. Yang, E. Farber, R. Lee, S. B. Buck, D. A. Andres, H. P. Spielmann, B. J. Agnew, F. Tamanoi, L. G. Fong, and S. G. Young. **Increasing the length of progerin's isoprenyl anchor does not worsen bone disease or survival in mice with Hutchinson-Gilford progeria syndrome.** *J. Lipid Res.* 2009. **50:** 126–134.

Hutchinson-Gilford progeria syndrome (HGPS) is a rare genetic disease characterized by a number of aging-like disease phenotypes (e.g., osteoporosis, loss of hair, reduced adipose tissue, occlusive vascular disease, and thin skin with a wizened appearance) (1, 2). HGPS is caused by point mutations in *LMNA*, the gene encoding prelamin A and lamin C (3). These point mutations alter splicing of the prelamin A pre-mRNA and lead to the production of a mutant prelamin A protein, commonly called progerin, containing an internal 50-amino-acid deletion (3). Progerin is targeted to the cell nucleus by a nuclear localization signal (4), and a significant amount of progerin is located at the rim of the nucleus adjacent to the inner nuclear membrane (5, 6). Progerin leads to dramatically misshapen cell nuclei (3, 5) and is responsible for all of the aging-like disease phenotypes in HGPS (3, 7).

Like wild-type prelamin A, progerin contains a carboxyl-terminal *CaaX* motif, which triggers farnesylation of the carboxyl-terminal cysteine (the "*C*" of the *CaaX* motif) (3). After endoproteolytic release of the last three amino acids of the protein (i.e., the *aaX* of the *CaaX* motif), the carboxyl-terminal farnesylcysteine is methylated (8, 9). Progerin lacks the sequences required for the ZMPSTE24-

Abbreviations: AG, anilinogeraniol; HGPS, Hutchinson-Gilford progeria syndrome; FTI, farnesyltransferase inhibitor; GGTI, geranylgeranyltransferase inhibitor; MEFs, mouse embryonic fibroblasts.
[1] To whom correspondence should be addressed.
e-mail: sgyoung@mednet.ucla.edu (S.G.Y.);
lfong@mednet.ucla.edu (L.G.F.)

This article is available online at http://www.jlr.org

mediated processing step that would ordinarily clip off the farnesylated and methylated cysteine and release mature lamin A (8). Thus, progerin terminates with a farnesyl-cysteine α-methyl ester (9). Progerin's carboxyl-terminal lipid anchor is thought to be important for targeting the protein to the inner nuclear membrane (5). When the farnesylation of progerin is blocked with a protein farnesyl-transferase inhibitor (FTI), progerin is mislocalized away from the nuclear rim and the frequency of misshapen nuclei is reduced (5). An FTI also ameliorates disease phenotypes in mouse models of progeria (7, 10, 11).

The fact that a farnesyl group would help to anchor progerin to the nuclear membrane is not surprising. In in vitro lipid bilayer studies, farnesylation of synthetic peptides increases their partitioning to the surface of phospholipids vesicles, proportionately reducing their concentration in the aqueous phase (12). On the other hand, it is important to emphasize that a farnesyl lipid is not a particularly strong membrane anchor. An *n*-alkyl chain with only 11 carbons is as effective as the 15-carbon branch-chain farnesyl group in promoting membrane binding (12). Also, a far-

nesyl lipid is only ~2% as potent as a 20-carbon geranyl-geranyl lipid in anchoring peptides to lipid membranes (12). The latter differences persist when the isoprenyl-cysteine is methylated (12).

Because the targeting of progerin to the nuclear rim is thought to be important in eliciting disease phenotypes in vivo and because a geranylgeranyl lipid is considerably stronger than a farnesyl group in promoting membrane binding, we hypothesized that a geranylgeranylated version of progerin would elicit more severe disease phenotypes than a farnesylated progerin. There is a straightforward path to examine this hypothesis. Gene-targeting approaches can be used to create mice expressing progerin (5, 7), and it is possible to trigger protein geranylgeranylation by altering the last amino acid of progerin's *CaaX* motif (13). In this study, we produced knock-in mice that expressed either a farnesylated or a geranylgeranylated version of progerin. Except for the length of the isoprenyl lipid anchor on the carboxyl-terminal cysteine of progerin, the two groups of mice were identical. We characterized both groups of mice, side-by-side, for severity of disease phenotypes.
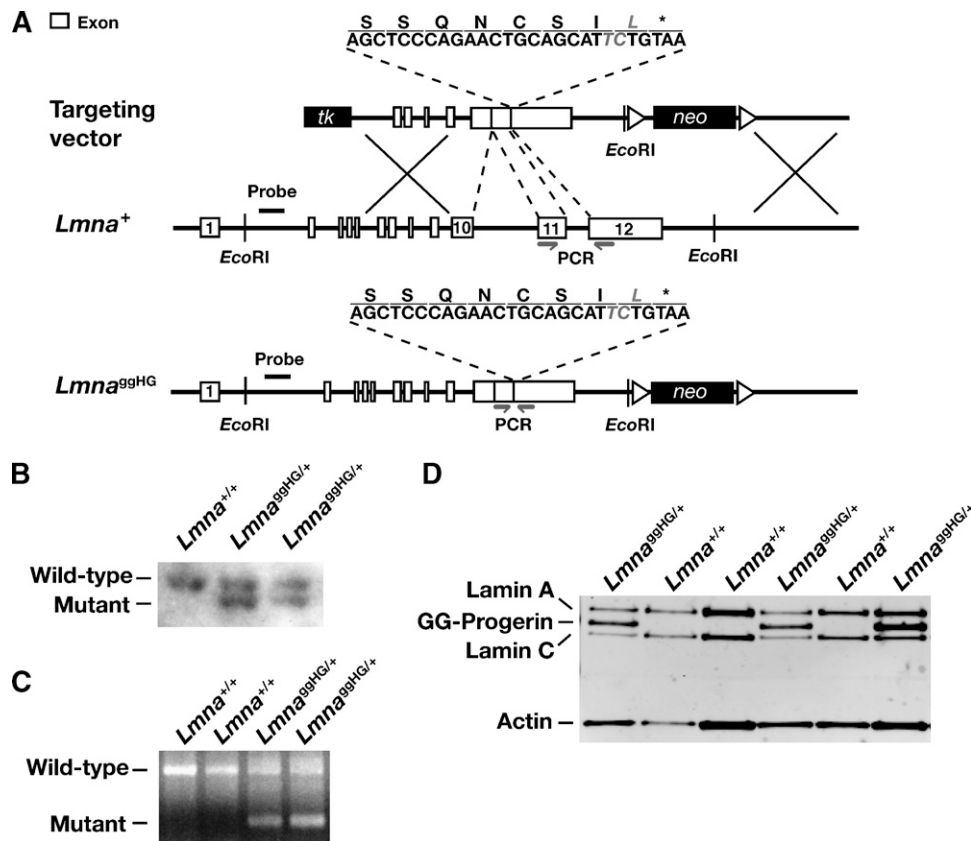

Fig. 1. Production of mice that express geranylgeranylated progerin. A: A mutant allele yielding geranyl-geranylated progerin, *Lmna*ggHG, was generated with a sequence-replacement vector that removes intron 10, intron 11, and the last 150 bp of exon 11, and introduces a point mutation in exon 12 that changes the methionine in the *CaaX* motif to leucine. B: Southern blot identification of the targeting event in two embryonic stem (ES) cell clones. The genomic DNA was cleaved with *Eco*RI, and the blot was hybridized with the 5′ flanking probe indicated in A. C: PCR strategy for genotyping *Lmna*ggHG/+ mice. Primers shown in A were used to amplify a 580-bp DNA fragment from the *Lmna*+ allele or a 185-bp fragment from the *Lmna*ggHG allele. D: Western blot identification of progerin in extracts of *Lmna*ggHG/+ mouse embryonic fibroblasts (MEFs), using a lamin A/C-specific polyclonal antibody.

MATERIALS AND METHODS

Knock-in mice expressing a geranylgeranylated version of progerin

To create a mutant *Lmna* allele yielding a geranylgeranylated progerin (*Lmna*^{ggHG}), we used a gene-targeting vector identical to one used previously to create a mutant allele yielding farnesylated progerin (*Lmna*^{HG}) (5), except for a point mutation in exon 12 (in the 5′ arm of the vector) that changes the methionine of progerin's *CaaX* motif to a leucine (i.e., CSIM to CSIL). The mutation was introduced into the 5′-arm of the vector by site-directed mutagenesis with the QuikChange kit (Stratagene, La Jolla, CA) and primer 5′-CTCCCAGAACTGCAGCATTCTG-TAATCTGGGACCTGCCAGG -3′ (and the complementary reverse primer). The integrity of the gene-targeting vector was verified by restriction endonuclease digestion and DNA sequencing (5).

After electroporating 129/OlaHsd embryonic stem cells with the gene-targeting vector, targeted clones were identified by Southern blotting with *Eco*RI-cleaved genomic DNA and a 348-bp 5′-flanking probe (5). Targeted ES cells were micro-injected into C57BL/6 blastocysts, and the resulting chimeras were bred with C57BL/6 females to generate *Lmna*$^{ggHG/+}$ mice. In parallel, *Lmna*$^{HG/+}$ ES cells (5, 7) were used to generate chimeras, which were bred to generate *Lmna*$^{HG/+}$ mice. Because *Lmna*$^{ggHG/+}$ and *Lmna*$^{HG/+}$ mice were generated from chimeras, they were identical (with one C57BL/6 chromosome and one 129/OlaHsd chromosome), except for the single-nucleotide difference in exon 12 of *Lmna*. Genotyping of mice was performed by PCR with genomic DNA from tail biopsies (5). The mice were fed a chow diet and housed in a virus-free barrier facility with a 12-h light-dark cycle. Body weights were measured weekly. All mouse experiments were approved by UCLA's Animal Research Committee.

Analysis of mouse embryonic fibroblasts

Primary mouse embryonic fibroblasts (MEFs) were prepared from E13.5 embryos (14), plated in 6-well plates, and grown to 75% confluency. To assess nuclear shape abnormalities, early-passage MEFs were grown on coverslips and then fixed and permeabilized as described previously (15). Cells were incubated with antibodies against lamin A (1:200, sc-20680, Santa Cruz Biotechnology, Santa Cruz, CA) for 2 h. After washing, cells were incubated with Alexa Fluor 568-conjugated anti-rabbit antibody (1:800, Jackson ImmunoResearch Laboratories, West Grove, PA) and DAPI to visualize DNA. Images were obtained on an Axiovert 200 MOT microscope (Carl Zeiss, Thornwood, NY), and nuclear shape (550–1,500 cells per genotype) was assessed in a blinded fashion (5, 16–18).

Metabolic labeling studies

To assess protein farnesylation, MEFs were incubated for 36 h with an analog of farnesol, 8-anilinogeraniol (AG) (30 μM in dimethyl sulfoxide) (19). AG is incorporated into anilinogeranyl diphosphate and used by protein farnesyltransferase as a substrate for the modification of *CaaX* proteins. The incorporation of AG into proteins can be detected by Western blotting with an AG-specific mouse monoclonal antibody (1:5,000) (19). To prepare samples for Western blots, the A-type lamins were immunoprecipitated with a goat anti-lamin A/C antibody (15 μl) (Santa Cruz Biotechnology) (20). Proteins were size-fractionated on 4–12% gradient polyacrylamide Bis-Tris gels (Invitrogen, Carlsbad, CA), and the separated proteins were transferred to nitrocellulose membranes for Western blotting. Signals were detected with an Odyssey infrared imaging scanner. The antibody dilutions were 1:200 for anti-lamin A/C goat IgG (sc-6215, Santa Cruz Bio-

technology), 1:5,000 for anti-AG mouse IgG, and 1:1,000 for anti-actin goat IgG (sc-1616, Santa Cruz Biotechnology). After washing the membranes, the membranes were incubated with 1:5,000 IRDye 800 anti-goat IgG and 1:5,000 IRDye 680 anti-mouse IgG (Li-Cor, Lincoln, NE).

Protein geranylgeranylation was assessed by azido geranyl-geranyl alcohol labeling. Cells were incubated with 50 μM azido
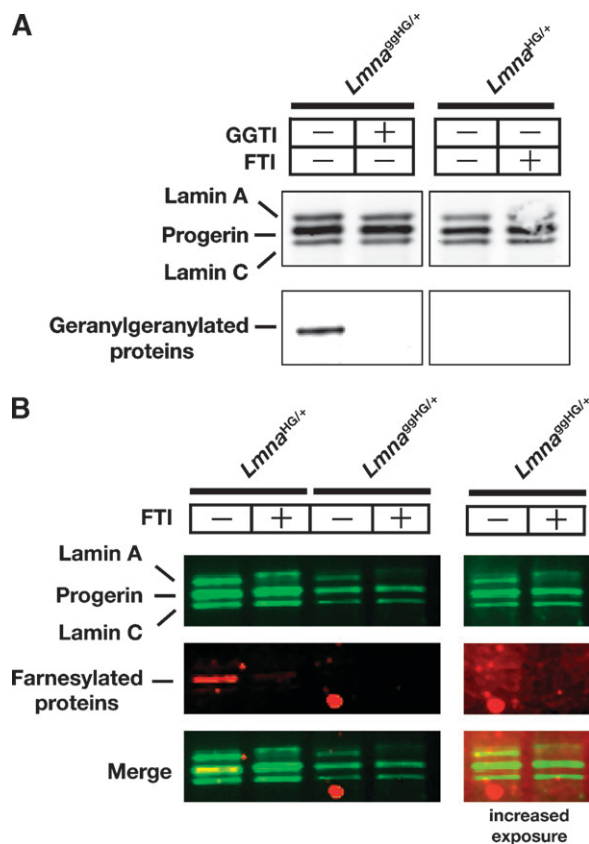

Fig. 2. Metabolic labeling studies to assess the farnesylation and geranylgeranylation of progerin in *Lmna*$^{ggHG/+}$ and *Lmna*$^{HG/+}$ MEFs. A: Assessing geranylgeranylation of progerin in *Lmna*$^{ggHG/+}$ fibroblasts. *Lmna*$^{ggHG/+}$ and *Lmna*$^{HG/+}$ MEFs were incubated with azido geranylgeranyl alcohol, which is used as a substrate by protein geranylgeranyltransferase, type I. To detect protein geranylgeranylation, extracts prepared from cells that had been incubated with azido geranylgeranyl alcohol and labeled with tetramethyl-rhodamine (TAMRA) with the Click-iT Tetramethylrhodamine (TAMRA) Protein Analysis Detection Kit were size-fractionated on a 4–12% polyacrylamide Bis-Tris gel. Geranylgeranylated proteins were then detected with a fluorescence imager. Next, the separated proteins were transferred to nitrocellulose and incubated with an antibody against lamin A/C, and a Western blot was performed with the Odyssey infrared scanner. B: Assessing farnesylation of progerin. Fibroblasts were incubated with anilinogeraniol (AG) (30 μM) in the presence (+) or absence (−) of a farnesyltransferase inhibitor (FTI) (ABT-100, 5 μM). Western blots were performed on cell extracts with an antibody specific for lamin A/C (green) and an antibody specific for AG (red). When progerin and lamin A/C were immunoprecipitated, the progerin in *Lmna*$^{HG/+}$ MEFs could be detected with an antibody against AG. As expected, the FTI blocked the incorporation of AG into progerin in *Lmna*$^{HG/+}$ MEFs. Because lower amounts of *Lmna*$^{ggHG/+}$ extracts were loaded (the last two lanes), these lanes are also shown at an increased exposure. Even with the longer exposure, no farnesylation of progerin in *Lmna*$^{ggHG/+}$ cells was detected. The electrophoretic mobility of progerin in *Lmna*$^{ggHG/+}$ and *Lmna*$^{HG/+}$ MEFs was identical.

geranylgeranyl alcohol for 48 h and harvested in 1% SDS and 50 mM Tris, pH 8. Protein extracts were prepared by sonication, chloroform-methanol precipitation, and resuspension in 1% SDS and 50 mM Tris, pH 8. Proteins that had incorporated azido geranylgeranyl alcohol were labeled with tetramethylrhodamine (TAMRA) with the Click-iT Tetramethylrhodamine (TAMRA) Protein Analysis Detection Kit (Invitrogen, Carlsbad, CA), according to the manufacturer's instructions. Proteins were size-fractionated on 4–12% gradient polyacrylamide Bis-Tris gels (Invitrogen), and labeled proteins were visualized with the Typhoon 9410 Variable Mode Imager (GE Healthcare, Piscataway, NJ). Following imaging, proteins were transferred to nitrocellulose for Western blotting with anti-lamin A/C goat IgG (sc-6215, Santa Cruz Biotechnology).
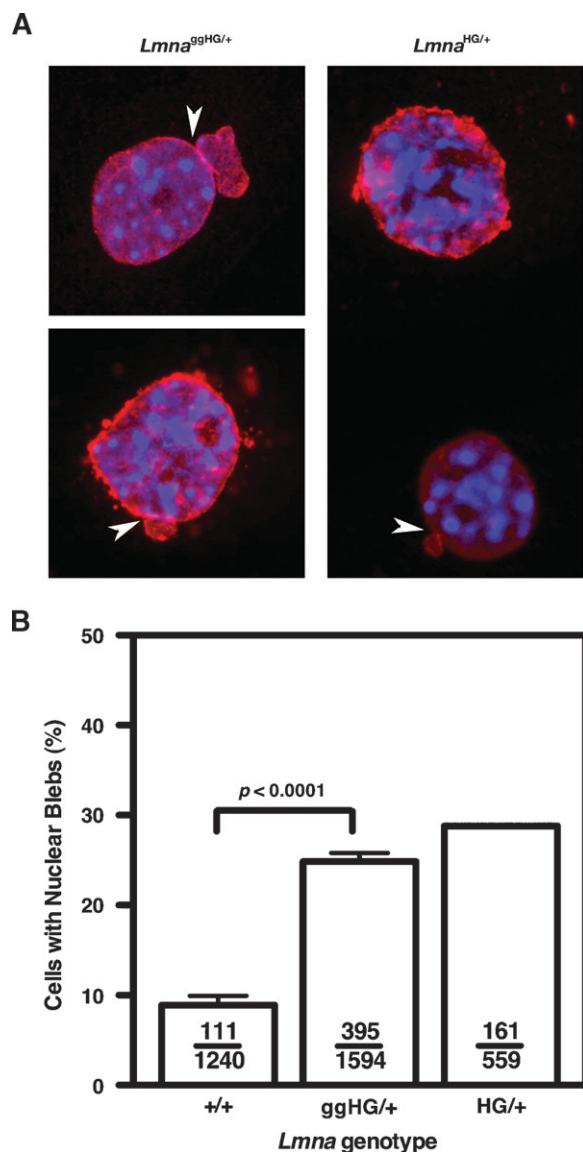
Fig. 3. Analysis of nuclear shape in $Lmna^{+/+}$, $Lmna^{ggHG/+}$, and $Lmna^{HG/+}$ MEFs. A: Immunostaining of $Lmna^{ggHG/+}$ and $Lmna^{HG/+}$ MEFs with a lamin A-specific antibody (red). Nuclei were counterstained with DAPI (blue). Blebs are indicated with white arrows. B: Percentage of cells containing misshapen nuclei in primary MEFs from $Lmna^{+/+}$, $Lmna^{ggHG/+}$, and $Lmna^{HG/+}$ embryos (n = 2–3 cell lines/genotype, $P < 0.0001$, χ^2 test). Ratios show the number of nuclear blebs over the total number of cells counted. Error bars indicate SEM.

Analysis of disease phenotypes

The interior of the thorax of $Lmna^{+/+}$, $Lmna^{ggHG/+}$, and $Lmna^{HG/+}$ mice was photographed, and the number of rib fractures was counted (7, 10, 11, 15, 18). The thoracic cages of $Lmna^{+/+}$, $Lmna^{ggHG/+}$, and $Lmna^{HG/+}$ mice were imaged by compact cone-beam tomography (μCT 40 scanner, Scanco Medical, Bassersdorf, Switzerland) (15, 17).

Protein extraction and Western blots

Urea-soluble extracts were prepared from early-passage MEFs and mouse tissues (21). Extracts were size-fractionated on 4–12% gradient polyacrylamide Bis-Tris gels (Invitrogen), and the separated proteins transferred to nitrocellulose membranes for Western blotting. Antibody dilutions were 1:200 for anti-lamin A/C goat IgG (sc-6215, Santa Cruz Biotechnology), 1:1,000 for anti-actin goat IgG (sc-1616, Santa Cruz Biotechnology), and 1:5,000 for IRDye 800 anti-goat IgG (Rockland Immunochemicals, Gilbertsville, PA). The IR-coupled antibodies were detected with an Odyssey infrared imaging scanner and quantified according to the manufacturer's instructions.

Extraction of RNA, cDNA synthesis, and RT-PCR

The isolation of RNA, cDNA synthesis, and RT-PCR were performed as described (18). Band intensities of the fragments amplified from $Lmna^{ggHG}$, $Lmna^{HG}$, and $Lmna^+$ transcripts were quantified with the Odyssey infrared imaging system and normalized to *36B4*.

Statistical analyses

The number of surviving male and female mice was recorded weekly. Differences were assessed with log-rank (Mantel-Cox) and Gehan-Breslow-Wilcoxon tests. Body weight curves were com-

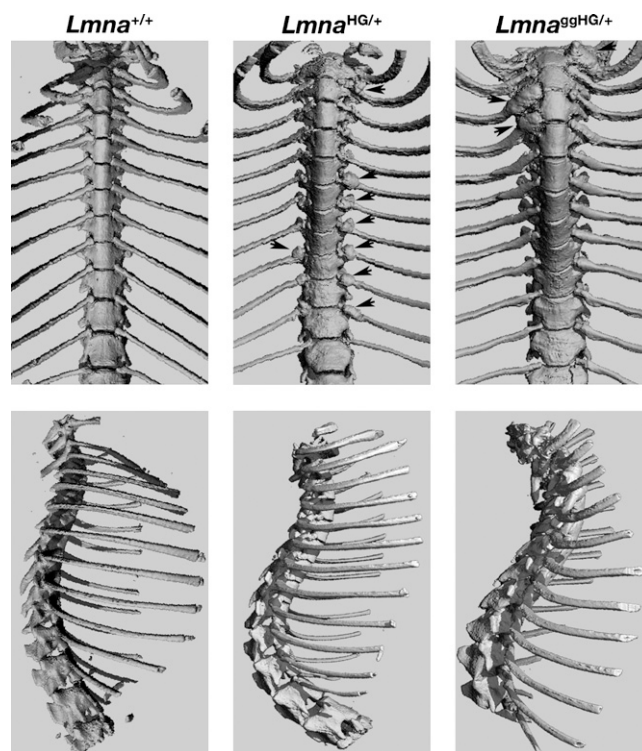**Fig. 4.** Surface renderings of μCT scans showing characteristic rib fractures in 6-month-old $Lmna^{ggHG/+}$ and $Lmna^{HG/+}$ mice. Arrowheads indicate rib fractures and surrounding callus.

Expression of Geranylgeranylated Progerin in Mice 129

pared with repeated-measures ANOVA. Differences in the number of rib fractures were assessed with a two-tailed Student's *t*-test. Differences in the percentages of misshapen nuclei were assessed with a χ^2 test.

RESULTS

We used gene targeting to create a mutant *Lmna* allele, $Lmna^{ggHG}$, that yields geranylgeranylated progerin (**Fig. 1A**). The $Lmna^{HG}$ allele is identical to the $Lmna^{HG}$ allele generated previously (5), except that the methionine in the *CaaX* motif was replaced with a leucine (a substitution that triggers protein geranylgeranylation). Multiple targeted ES cell clones were identified by Southern blotting (Fig. 1B), and two were used to create male chimeric mice, which were bred with C57BL/6 females to produce heterozygous knock-in mice ($Lmna^{ggHG/+}$). Offspring were genotyped by PCR (Fig. 1C). As expected, fibroblasts from $Lmna^{ggHG/+}$ embryos produced substantial amounts of progerin protein (Fig. 1D).

The carboxyl-terminal leucine in the progerin of $Lmna^{ggHG/+}$ mice was predicted to trigger protein geranylgeranylation. Indeed, metabolic labeling studies revealed that the progerin in $Lmna^{ggHG/+}$ MEFs, but not $Lmna^{HG/+}$ MEFs, was geranylgeranylated (**Fig. 2A**). As expected, the progerin in $Lmna^{HG/+}$ MEFs was farnesylated, as judged by metabolic labeling with a farnesol analog (Fig. 2B). We could not detect farnesylation of progerin in $Lmna^{ggHG/+}$ MEFs (Fig. 2B).

Progerin's lipid anchor is important both for the misshapen nuclei phenotype in cultured fibroblasts and disease phenotypes in mice (5, 7). Because a geranylgeranyl anchor binds to membranes more avidly than a farnesyl anchor, we suspected that $Lmna^{ggHG/+}$ mice would exhibit more severe phenotypes than $Lmna^{HG/+}$ mice. As expected, $Lmna^{ggHG/+}$ MEFs (n = 3 independent cell lines) exhibited a high frequency of misshapen nuclei (**Fig. 3A**), but to our surprise, the frequency of the misshapen nuclei was not greater than in $Lmna^{HG/+}$ MEFs (Fig. 3B).

One of the most easily quantifiable disease phenotypes in mouse models of progeria is bone fractures at the sites of osteolytic lesions in the ribs (which occur adjacent to the costovertebral joints). The number of rib fractures increases with age (7). The rib factures heal poorly, so each fracture can be easily detected by exuberant fracture callus (7, 11, 14, 15, 17, 18). All $Lmna^{ggHG/+}$ and $Lmna^{HG/+}$ mice developed rib fractures, which were easily detectable by
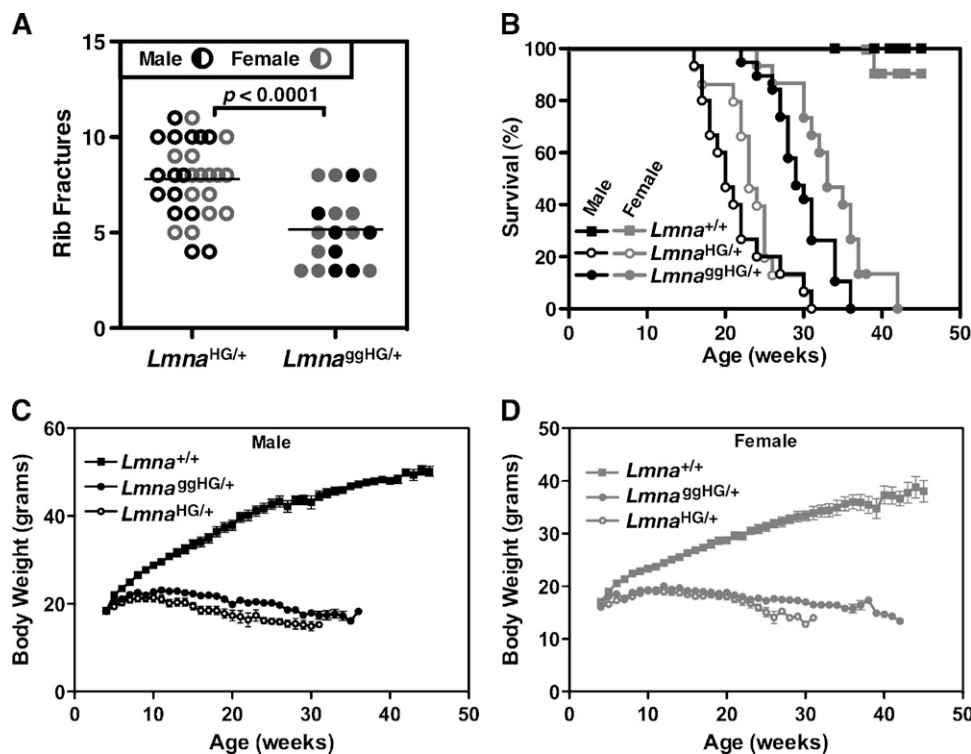
Fig. 5. Phenotypes of $Lmna^{ggHG/+}$ mice. A: Number of rib fractures in $Lmna^{ggHG/+}$ mice (n = 7 males, 11 females) and $Lmna^{HG/+}$ mice (n = 15 males, 15 females). The number of fractures was lower in $Lmna^{ggHG/+}$ mice than in $Lmna^{HG/+}$ mice ($P < 0.0001$), despite the fact that $Lmna^{ggHG/+}$ mice were far older than the $Lmna^{HG/+}$ mice (32.35 ± 4.96 weeks vs. 22.47 ± 4.44 weeks). B: Kaplan-Meier survival plots for $Lmna^{ggHG/+}$ mice (n = 19 males, 15 females), $Lmna^{HG/+}$ mice (n = 15 males, 15 females), and $Lmna^{+/+}$ mice (n = 16 males, 14 females). Male and female $Lmna^{ggHG/+}$ mice survived significantly longer than $Lmna^{HG/+}$ mice ($P < 0.0001$). C: Body weight curves of male $Lmna^{HG/+}$ (n = 15), $Lmna^{+/+}$ (n = 16), and $Lmna^{ggHG/+}$ mice (n = 19). D: Body weight curves of female $Lmna^{HG/+}$ (n = 15), $Lmna^{+/+}$ (n = 14), and $Lmna^{ggHG/+}$ mice (n = 15). Body weights tended to be higher in male and female $Lmna^{ggHG/+}$ mice than in $Lmna^{HG/+}$ mice, but this difference was not statistically significant.

μCT scanning (**Fig. 4**). However, contrary to our expectations, the number of rib fractures in $Lmna^{ggHG/+}$ mice was lower than in $Lmna^{HG/+}$ mice ($P < 0.0001$), despite the fact that $Lmna^{ggHG/+}$ mice were significantly older than the $Lmna^{HG/+}$ mice when the fractures were counted (32.35 ± 4.96 weeks vs. 22.47 ± 4.44 weeks) (**Fig. 5A**). The survival of $Lmna^{ggHG/+}$ mice, both males and females, was better than $Lmna^{HG/+}$ mice, as judged by Kaplan-Meier analysis ($P < 0.0001$ for both males and females) (Fig. 5B). Compared with wild-type mice, both $Lmna^{ggHG/+}$ and $Lmna^{HG/+}$ mice exhibited profoundly abnormal body weight curves ($P < 0.0001$ for both groups) (Fig. 5C, D). In line with the differences in rib fractures and survival, body weights tended to be higher in $Lmna^{ggHG/+}$ mice than in $Lmna^{HG/+}$ mice (Fig. 5C, D), although these differences did not achieve statistical significance.

Disease phenotypes were less severe in $Lmna^{ggHG/+}$ mice (Fig. 5), even though the progerin contained a lipid anchor with a greater avidity for membrane surfaces. We hypothesized that one potential explanation for this finding would be lower steady-state levels of progerin in $Lmna^{ggHG/+}$ mice. To test this hypothesis, Western blots were performed on tissue extracts of $Lmna^{HG/+}$ and $Lmna^{ggHG/+}$ mice, and the progerin and lamin C bands were quantified with the Odyssey infrared scanner. Levels of progerin, relative to lamin C, were lower in $Lmna^{ggHG/+}$ tissues (heart, liver, kidney, skull) than in $Lmna^{HG/+}$ tissues (**Fig. 6A–D, F**), though the difference in progerin lev-

els in kidney were only evident with quantification of the band intensities on the Western blots. Progerin levels, relative to lamin C, tended to be somewhat lower in $Lmna^{ggHG/+}$ MEFs, although this difference did not achieve statistical significance (Fig. 6E, F). The differences in progerin levels in $Lmna^{ggHG/+}$ and $Lmna^{HG/+}$ tissues could not be ascribed to differences in the levels of progerin transcripts. For example, progerin transcript levels in the heart, as judged by RT-PCR, were not different in $Lmna^{ggHG/+}$ and $Lmna^{HG/+}$ mice (**Fig. 7A, B**).

DISCUSSION

In 1988, Clarke et al. (22) proposed that $CaaX$ motifs represented a potential signal for protein lipidation and methylation. In the next few years, it became clear that certain $CaaX$ proteins are farnesylated (23), whereas others are geranylgeranylated (24). The different isoprenyl lipid anchors have dramatically different properties in lipid partitioning assays, with the geranylgernayl lipid being ~45-fold more potent in promoting associations with membrane surfaces (12). However, the importance of a farnesyl versus a geranylgeranyl lipid anchor has never been investigated in vivo, for any of the dozens of farnesylated and geranylgeranylated proteins within cells. In the current study, we addressed this issue, focusing on a farnesylated $CaaX$ protein, progerin, which is the culprit molecule in
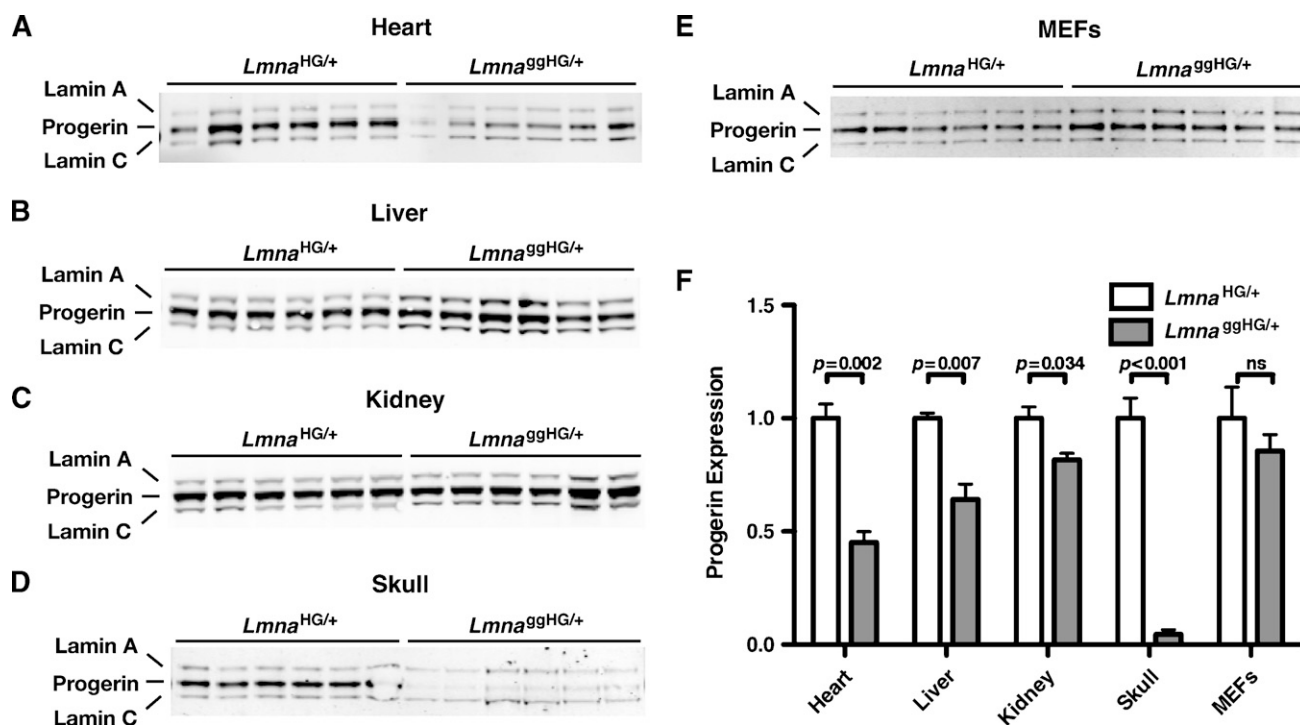

Fig. 6. Western blots showing relative levels of progerin in the tissues of $Lmna^{HG/+}$ and $Lmna^{ggHG/+}$ mice and in $Lmna^{HG/+}$ and $Lmna^{ggHG/+}$ MEFs. A–E: Western blots (with an antibody against lamin A/C) showing progerin, lamin A, and lamin C in the heart (A), liver (B), kidney (C), and skull (D) of $Lmna^{HG/+}$ and $Lmna^{ggHG/+}$ mice (n = 3/genotype, each sample in duplicate). E: Western blot (with an antibody against lamin A/C) showing progerin, lamin A, and lamin C in $Lmna^{HG/+}$ and $Lmna^{ggHG/+}$ MEFs (n = 3 cell lines/genotype, each sample in duplicate). F: Quantitative analysis of progerin expression in the tissues and MEFs of $Lmna^{HG/+}$ and $Lmna^{ggHG/+}$ mice. Progerin/lamin C ratios in $Lmna^{ggHG/+}$ samples are expressed relative to those in $Lmna^{HG/+}$ samples (which were set at a value of one).
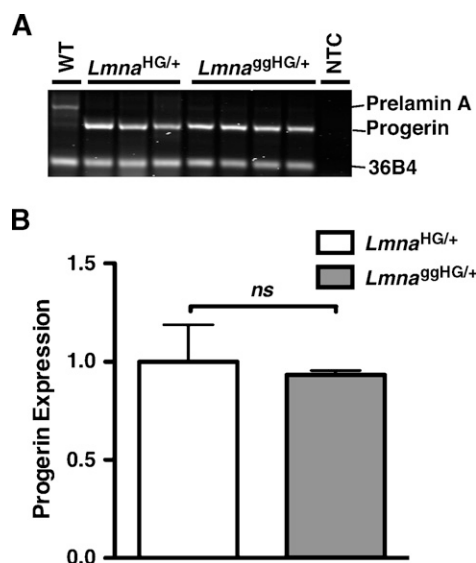
Fig. 7. Progerin transcript levels in heart RNA from $Lmna^{HG/+}$ (n = 3) and $Lmna^{ggHG/+}$ mice (n = 4). A: Syto-60-stained agarose gel of RT-PCR products (at cycle 20) from RNA prepared from $Lmna^{HG/+}$ and $Lmna^{ggHG/+}$ mice. The RT-PCR reaction spanned sequences encoded by exons 10–12 of $Lmna$. Image intensity was quantified with the Odyssey infrared imaging system. $36B4$ was used as an internal control. WT, wild-type; NTC, no template control. B: Quantitative analysis of progerin mRNA levels, corrected for $36B4$ expression. Progerin mRNA levels in $Lmna^{ggHG/+}$ samples were expressed relative to those in $Lmna^{HG/+}$ samples (which were set at a value of one).

HGPS. Because targeting of progerin to the nuclear rim is widely assumed to be important for disease pathogenesis (5, 8, 15, 16, 25), we reasoned that progerin containing the stronger geranylgeranyl lipid anchor might elicit more severe disease phenotypes. To examine this issue, we generated a new line of knock-in mice expressing geranylgeranylated progerin. We then examined, side-by-side, mice expressing progerin terminating with a farnesylcysteine ($Lmna^{HG/+}$) and mice expressing progerin terminating with a geranylgeranylcysteine ($Lmna^{ggHG/+}$). Aside from the length of the isoprenyl lipid attached to progerin, these mice were identical. The $Lmna^{ggHG/+}$ MEFs exhibited a high frequency of misshapen nuclei, but no higher than in $Lmna^{HG/+}$ MEFs. Contrary to our hypothesis, the severity of disease phenotypes was reduced in $Lmna^{ggHG/+}$ mice. Male and female $Lmna^{ggHG/+}$ mice survived longer than $Lmna^{HG/+}$ mice, and the number of rib fractures was lower in $Lmna^{ggHG/+}$ mice. This latter finding was convincing, given that rib fractures increase steadily with age (7), and the $Lmna^{ggHG/+}$ mice were considerably older than the $Lmna^{HG/+}$ mice at the time that the rib fractures were counted.

What might explain the milder phenotype in $Lmna^{ggHG/+}$ mice? We reasoned that different steady-state levels of progerin in the two models might conceivably underlie the phenotypic differences. Indeed, levels of progerin were lower in $Lmna^{ggHG/+}$ mice, and this difference was striking in certain tissues, for example the skull and the heart. The proposition that different steady-state levels of progerin might explain the phenotypic differences is plausible. In humans, $LMNA$ mutations yielding particularly high levels of progerin expression are associated with more severe forms of progeria (26). Also, we showed that $Lmna^{HG/LCO}$ mice (mice with one $Lmna^{HG}$ allele and one "lamin C-only" allele) exhibit lower tissue levels of progerin than $Lmna^{HG/+}$ mice, despite identical levels of progerin transcripts. The lower steady-state progerin levels in $Lmna^{HG/LCO}$ mice were accompanied by reduced disease phenotypes (18). Given that progerin transcript levels in $Lmna^{ggHG/+}$ and $Lmna^{HG/+}$ mice are identical, we presume that the geranylgeranyl lipid anchor increases the turnover of progerin. This possibility is not farfetched. Perturbed levels of prenylated proteins in cells have been observed when protein prenylation is altered (27, 28). Although less likely, it is conceivable that the geranylgeranylated form of progerin interacts differently with other nuclear envelope proteins, and that this, rather than lower steady-state progerin levels, is responsible for the milder disease phenotypes.

When evaluating the impact of gene-targeted mutations in F2 mice on a mixed genetic background, one needs to be concerned about the effects of "passenger genes" on phenotypes (29). That concern does not apply to the current experiments, in which we studied F1 mice bred from chimeras (which were created from the same strain of ES cells). Aside from the single amino acid substitution in newly synthesized progerin and the length of the isoprenyl anchor in the fully processed progerin, both groups of mice were genetically identical, with each mouse having one 129/OlaHsd chromosome and one C57BL/6 chromosome. Because the mice were genetically identical (aside from the targeted mutation), we are confident that the phenotypic differences are due to the effects of the targeted mutation. Another reason for confidence is that we observed the same phenotype in independent lines of $Lmna^{ggHG/+}$ mice generated from independently targeted ES cells.

Although this study is the first to examine the in vivo impact of an "isoprenyl anchor substitution," earlier studies with model organisms and cultured mammalian cells had suggested that an isoprenyl anchor substitution could have biological consequences. In 1980, Fujino and Kitada (30) examined the impact of isoprenyl chain length on the potency of a normally farnesylated mating pheromone from $Tremella mesenterica$. They found that chemically synthesized mating pheromone peptides with isoprenyl chain lengths of 20 or 25 carbons were far more potent in stimulating mating than the 15-carbon farnesylated peptide (30). Cox et al. (31) found that a geranylgeranylated Ras had the same transforming properties as farnesylated Ras, but the geranylgeranylated Ras appeared to be more potent in inhibiting the growth of nontransformed 3T3 cells. Also, Matsuda et al. (32) reported that a geranylgeranylated version of the heterotrimeric G-protein γ-subunit bound membranes more avidly than the farnesylated protein and was more potent in promoting pertussis toxin-catalyzed ADP ribosylation of transducin-α. Unfortunately, neither of the aforementioned mammalian cell-culture stud-

ies (31, 32) examined the impact of the different isoprenyl anchors on the steady-state level of the prenylated protein.

In our studies, we created mice containing a leucine rather than a methionine in the "X" position of the *CaaX* motif, a substitution that triggers protein geranylgeranylation by protein geranylgeranyltransferase, type 1. While we had little doubt that the methionine-to-leucine substitution would trigger geranylgeranylation, we were delighted to confirm this finding with new metabolic labeling tools. To assess protein geranylgeranylation, we labeled cells with azido geranylgeranyl alcohol, immunoprecipitated the A-type lamins, and detected via a "Click Chemistry" reaction with TAMRA-alkyne dye (33, 34). After separating the proteins by gel electrophoresis, labeled proteins were visualized with the Typhoon 9410 Variable Mode Imager. As expected, the progerin in $Lmna^{ggHG/+}$ cells, but not $Lmna^{HG/+}$ cells, was geranylgeranylated. At the same time, labeling of cells with a farnesol analog revealed that progerin in $Lmna^{HG/+}$ cells was farnesylated. We expect that these new labeling tools will be useful to those interested in the prenylation of lamins. A recent study from Europe (35) raised the possibility that prelamin A might be alternately geranylgeranylated when cells are treated with a farnesyltransferase inhibitor (FTI). In the case of another *CaaX* protein that terminates in methionine, K-Ras, alternate prenylation in the setting of FTI treatment has been well documented (36). In the future, metabolic labeling studies should be helpful in determining whether alternate prenylation of prelamin A, progerin, and the B-type lamins occurs and in gauging the extent of alternate prenylation under different circumstances. Also, these metabolic labeling tools will be useful for defining the specificity of commonly used inhibitors of protein prenylation.

In summary, we found no support for our original hypothesis, which is that the substitution of a geranylgeranyl lipid for progerin's farnesyl lipid anchor would worsen disease phenotypes. Instead, geranylgeranylated progerin yielded milder disease phenotypes, likely because this substitution results in lower steady-state levels of progerin. These results indicate that the strength of the isoprenyl anchor in binding to membrane surfaces may not be the dominant factor in the emergence of the disease phenotypes of progeria, and that other properties of progerin, for example abnormal protein-protein interactions, could be more important. Along these lines, a recent study concluded that progerin formed abnormal heterodimers with the B-type lamins (37). We suspect that this type of abnormal protein-protein interaction could ultimately prove to be more relevant to disease pathogenesis than the degree of hydrophobicity of the isoprenyl lipid anchor.

REFERENCES

1. Debusk, F. L. 1972. The Hutchinson-Gilford progeria syndrome. *J. Pediatr.* **80:** 697–724.

2. Merideth, M. A., L. B. Gordon, S. Clauss, V. Sachdev, A. C. Smith, M. B. Perry, C. C. Brewer, C. Zalewski, H. J. Kim, B. Solomon, et al. 2008. Phenotype and course of Hutchinson-Gilford progeria syndrome. *N. Engl. J. Med.* **358:** 592–604.

3. Eriksson, M., W. T. Brown, L. B. Gordon, M. W. Glynn, J. Singer, L. Scott, M. R. Erdos, C. M. Robbins, T. Y. Moses, P. Berglund, et al. 2003. Recurrent de novo point mutations in lamin A cause Hutchinson–Gilford progeria syndrome. *Nature.* **423:** 293–298.

4. Lin, F., and H. J. Worman. 1993. Structural organization of the human gene encoding nuclear lamin A and nuclear lamin C. *J. Biol. Chem.* **268:** 16321–16326.

5. Yang, S. H., M. O. Bergo, J. I. Toth, X. Qiao, Y. Hu, S. Sandoval, M. Meta, P. Bendale, M. H. Gelb, S. G. Young, et al. 2005. Blocking protein farnesyltransferase improves nuclear blebbing in mouse fibroblasts with a targeted Hutchinson-Gilford progeria syndrome mutation. *Proc. Natl. Acad. Sci. USA.* **102:** 10291–10296.

6. Goldman, R. D., D. K. Shumaker, M. R. Erdos, M. Eriksson, A. E. Goldman, L. B. Gordon, Y. Gruenbaum, S. Khuon, M. Mendez, R. Varga, et al. 2004. Accumulation of mutant lamin A causes progressive changes in nuclear architecture in Hutchinson-Gilford progeria syndrome. *Proc. Natl. Acad. Sci. USA.* **101:** 8963–8968.

7. Yang, S. H., M. Meta, X. Qiao, D. Frost, J. Bauch, C. Coffinier, S. Majumdar, M. O. Bergo, S. G. Young, and L. G. Fong. 2006. Treatment with a protein farnesyltransferase inhibitor improves disease phenotypes in mice with a targeted Hutchinson-Gilford progeria syndrome mutation. *J. Clin. Invest.* **116:** 2115–2121.

8. Young, S. G., L. G. Fong, and S. Michaelis. 2005. Prelamin A, Zmpste24, misshapen cell nuclei, and progeria—New evidence suggesting that protein farnesylation could be important for disease pathogenesis. *J. Lipid Res.* **46:** 2531–2558.

9. Dechat, T., T. Shimi, S. A. Adam, A. E. Rusinol, D. A. Andres, H. P. Spielmann, M. S. Sinensky, and R. D. Goldman. 2007. Alterations in mitosis and cell cycle progression caused by a mutant lamin A known to accelerate human aging. *Proc. Natl. Acad. Sci. USA.* **104:** 4955–4960.

10. Fong, L., D. Frost, M. Meta, X. Qiao, S. Yang, C. Coffinier, and S. Young. 2006. A protein farnesyltransferase inhibitor ameliorates disease in a mouse model of progeria. *Science.* **311:** 1621–1623.

11. Yang, S. H., X. Qiao, L. G. Fong, and S. G. Young. 2008. Treatment with a farnesyltransferase inhibitor improves survival in mice with a Hutchinson-Gilford progeria syndrome mutation. *Biochim. Biophys. Acta.* **1781:** 36–39.

12. Silvius, J. R., and F. l'Heureux. 1994. Fluorimetric evaluation of the affinities of isoprenylated peptides for lipid bilayers. *Biochemistry.* **33:** 3014–3022.

13. Zhang, F. L., and P. J. Casey. 1996. Protein prenylation: molecular mechanisms and functional consequences. *Annu. Rev. Biochem.* **65:** 241–269.

14. Bergo, M. O., B. Gavino, J. Ross, W. K. Schmidt, C. Hong, L. V. Kendall, A. Mohr, M. Meta, H. Genant, Y. Jiang, et al. 2002. *Zmpste24* deficiency in mice causes spontaneous bone fractures, muscle weakness, and a prelamin A processing defect. *Proc. Natl. Acad. Sci. USA.* **99:** 13049–13054.

15. Fong, L. G., J. K. Ng, M. Meta, N. Cote, S. H. Yang, C. L. Stewart, T. Sullivan, A. Burghardt, S. Majumdar, K. Reue, et al. 2004. Heterozygosity for Lmna deficiency eliminates the progeria-like phenotypes in Zmpste24-deficient mice. *Proc. Natl. Acad. Sci. USA.* **101:** 18111–18116.

16. Toth, J. I., S. H. Yang, X. Qiao, A. P. Beigneux, M. H. Gelb, C. L. Moulson, J. H. Miner, S. G. Young, and L. G. Fong. 2005. Blocking protein farnesyltransferase improves nuclear shape in fibroblasts from humans with progeroid syndromes. *Proc. Natl. Acad. Sci. USA.* **102:** 12873–12878.

17. Fong, L. G., J. K. Ng, J. Lammerding, T. A. Vickers, M. Meta, N. Cote, B. Gavino, X. Qiao, S. Y. Chang, S. R. Young, et al. 2006. Prelamin A and lamin A appear to be dispensable in the nuclear lamina. *J. Clin. Invest.* **116:** 743–752.

18. Yang, S. H., X. Qiao, E. Farber, S. Y. Chang, L. G. Fong, and S. G. Young. 2008. Eliminating the synthesis of mature lamin A reduces disease phenotypes in mice carrying a Hutchinson-Gilford progeria syndrome allele. *J. Biol. Chem.* **283:** 7094–7099.

19. Troutman, J. M., M. J. Roberts, D. A. Andres, and H. P. Spielmann. 2005. Tools to analyze protein farnesylation in cells. *Bioconjug. Chem.* **16:** 1209–1217.

20. Coffinier, C., S. E. Hudon, R. Lee, E. A. Farber, C. Nobumori, J. H. Miner, D. A. Andres, H. P. Spielmann, C. A. Hrycyna, L. G. Fong, et al. 2008. A potent HIV protease inhibitor, darunavir, does not

inhibit ZMPSTE24 or lead to an accumulation of farnesyl-prelamin A in cells. *J. Biol. Chem.* **283:** 9797–9804.

21. Dalton, M., and M. Sinensky. 1995. Expression systems for nuclear lamin proteins: farnesylation in assembly of nuclear lamina. *In* Methods Enzymol. J. C. Patrick and E. B. Janice, editors. Academic Press. 134–148.

22. Clarke, S., J. P. Vogel, R. J. Deschenes, and J. Stock. 1988. Posttranslational modification of the Ha-*ras* oncogene protein: evidence for a third class of protein carboxyl methyltransferases. *Proc. Natl. Acad. Sci. USA.* **85:** 4643–4647.

23. Farnsworth, C. C., S. L. Wolda, M. H. Gelb, and J. A. Glomset. 1989. Human lamin B contains a farnesylated cysteine residue. *J. Biol. Chem.* **264:** 20422–20429.

24. Yamane, H. K., C. C. Farnsworth, H. Xie, W. Howald, B. K-K. Fung, S. Clarke, M. H. Gelb, and J. A. Glomset. 1990. Brain G protein γ subunits contain an all-*trans*-geranylgeranyl-cysteine methyl ester at their carboxyl termini. *Proc. Natl. Acad. Sci. USA.* **87:** 5868–5872.

25. Meta, M., S. H. Yang, M. O. Bergo, L. G. Fong, and S. G. Young. 2006. Protein farnesyltransferase inhibitors and progeria. *Trends Mol. Med.* **12:** 480–487.

26. Moulson, C. L., L. G. Fong, J. M. Gardner, E. A. Farber, G. Go, A. Passariello, D. K. Grange, S. G. Young, and J. H. Miner. 2007. Increased progerin expression associated with unusual LMNA mutations causes severe progeroid syndromes. *Hum. Mutat.* **28:** 882–889.

27. Seabra, M. C., Y. K. Ho, and J. S. Anant. 1995. Deficient geranyl-geranylation of Ram/Rab27 in choroideremia. *J. Biol. Chem.* **270:** 24420–24427.

28. Storch, S., S. Pohl, A. Quitsch, K. Falley, and T. Braulke. 2007. C-terminal prenylation of the CLN3 membrane glycoprotein is required for efficient endosomal sorting to lysosomes. *Traffic.* **8:** 431–444.

29. Smithies, O., and N. Maeda. 1995. Gene targeting approaches to complex genetic diseases: atherosclerosis and essential hypertension. *Proc. Natl. Acad. Sci. USA.* **92:** 5266–5272.

30. Fujino, M., and C. Kitada. 1980. Biological activity of synthetic analogs of tremeogen A-10. *Naturwissenschaften.* **67:** 406–408.

31. Cox, A. D., M. M. Hisaka, J. E. Buss, and C. J. Der. 1992. Specific isoprenoid modification is required for function of normal, but not oncogenic, Ras protein. *Mol. Cell. Biol.* **12:** 2606–2615.

32. Matsuda, T., Y. Hashimoto, H. Ueda, T. Asano, Y. Matsuura, T. Doi, T. Takao, Y. Shimonishi, and Y. Fukada. 1998. Specific isoprenyl group linked to transducin gamma-subunit is a determinant of its unique signaling properties among G-proteins. *Biochemistry.* **37:** 9843–9850.

33. Kolb, H., M. Finn, and K. Sharpless. 2001. Click Chemistry: diverse chemical function from a few good reactions. *Angew. Chem.* **40:** 2004–2021.

34. Tornoe, C. W., C. Christensen, and M. Meldal. 2002. Peptidotriazoles on solid phase: [1,2,3]-triazoles by regiospecific copper(i)-catalyzed 1,3-dipolar cycloadditions of terminal alkynes to azides. *J. Org. Chem.* **67:** 3057–3064.

35. Varela, I., S. Pereira, A. P. Ugalde, C. L. Navarro, M. F. Suarez, P. Cau, J. Cadinanos, F. G. Osorio, N. Foray, J. Cobo, et al. 2008. Combined treatment with statins and aminobisphosphonates extends longevity in a mouse model of human premature aging. *Nat. Med.* **14:** 767–772.

36. Whyte, D. B., P. Kirschmeier, T. N. Hockenberry, I. Nunez-Oliva, L. James, J. J. Catino, W. R. Bishop, and J-K. Pai. 1997. K- and N-Ras are geranylgeranylated in cells treated with farnesyl protein transferase inhibitors. *J. Biol. Chem.* **272:** 14459–14464.

37. Delbarre, E., M. Tramier, M. Coppey-Moisan, C. Gaillard, J. C. Courvalin, and B. Buendia. 2006. The truncated prelamin A in Hutchinson-Gilford progeria syndrome alters segregation of A-type and B-type lamin homopolymers. *Hum. Mol. Genet.* **15:** 1113–1122.